



Sol gel dip coated tin oxide thin films

G.Ramanathan¹, R.John Xavier² and K.R.Murali³¹Department of physics, Sri Sairam Engineering College, Chennai, India.²Department of Physics, Periyar E.V.R College, Trichy, India.³ECMS Division, CSIR-CECRI, Karaikudi, India.

ARTICLE INFO

Article history:

Received: 1 August 2012;

Received in revised form:

31 August 2012;

Accepted: 20 September 2012;

Keywords

Thin films,
Semiconductor,
Sol gel.

ABSTRACT

Tin Oxide thin films were deposited by sol gel dip coating method using the acrylamide route. The films were post heated at different temperature in the range of 350-525 °C. X-Ray diffraction (XRD) studies indicated the formation of tetragonal SnO₂. The Optimum temperature for the formation of the films was 450 °C. Microstructural parameters were estimated from the XRD data. XPS studies indicated the peaks corresponding to Sn 3d and O1s. Transmission spectra exhibited interference fringes. Refractive Index was in the range of 2.05-2.18. Optical bandgap value was around 3.68 eV. Three fundamental Raman lines are observed which agree well with that of the bulk material.

© 2012 Elixir All rights reserved.

Introduction

Transparent conducting oxide films (TCOs) have been studied for many years due to their low resistivity [1] and high optical transparency [2] in the visible region. Among the available TCOs, tin oxide (SnO₂) films have been widely used as transparent conducting electrodes in many optoelectronic and electro-optic devices such as solar cells and flat panel displays. In addition, SnO₂ has a wide band gap of 3.6–4.0eV [3–5] and many advantages like a low growth temperature and high chemical stability compared with other materials. Due to the intrinsic defects such as oxygen vacancy, interstitial tin, and so on, the unintentionally doped SnO₂ thin film shows n-type conduction, which constrains its applications badly. In the theoretical study by SnO₂ or doped SnO₂ thin films have been prepared by many techniques, such as electrostatic spray deposition [6], pulsed-laser deposition [7,8], laser chemical vapor deposition [9] and sol–gel [10,11]. In this work, SnO₂ thin films have been deposited by the sol gel dip coating method using Acrylamide precursors. The films were then characterized by x-ray diffraction using Phillips x-ray unit and CuK α radiation. Optical transmission spectra were recorded using U3400 Hitachi UV-Vis-NIR spectrophotometer. Transport parameters were determined by Hall measurements. The resistivity of the films was estimated by the four probe technique. Laser Raman studies were made using Renishaw Invia laser Raman microscope with 633 nm 18 mW He-Ne laser.

Results and discussion

XRD patterns of the films heat treated at different temperatures on the range of 350 - 525°C is shown in Fig.1. Peaks corresponding to single phase tetragonal rutile structure of SnO₂ are observed in all the cases. The peaks corresponding to the (110), (101), (200), (211) and (002) are observed in all cases. It is observed that the width of the peaks decreases and height of the peaks increases with increase of post heat treatment temperature. The grain size increases from 10 nm to 25nm with increase of heat treatment temperature. The films could not be heat treated at temperatures higher than 500°C, because glass

substrates have been used for depositing the films and the glass bends beyond 525°C.

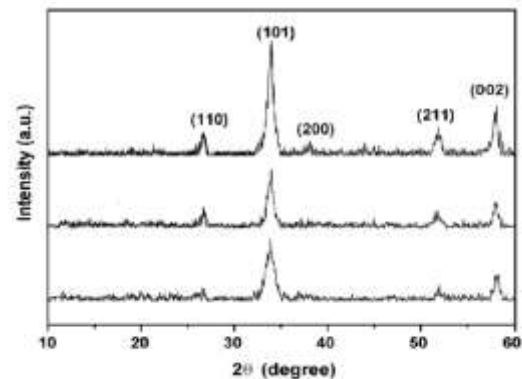


Fig.1 – XRD patterns of SnO₂ films heat treated at different temperatures (a) 350°C (b) 450°C (c) 525°C

The lattice constant 'a' and 'c', for the tetragonal phase structure is determined by the relation

$$1/d^2 = (h^2 + k^2)/a^2 + l^2/c^2 \dots\dots\dots(1)$$

Where 'd' is the interplaner distance and (hkl) are miller indices, respectively. The lattice constants 'a' and 'c' are calculated and given in Table 1. The average grain size of the SnO₂ thin films were estimated for all the observed planes by using Scherrer's formula [12].

$$D = k\lambda / \beta \cos\theta \dots\dots\dots(2)$$

Where 'k' varies from 0.89 to 1.39. But in most of the cases it is closer to 1. Hence for grain size calculation it is taken as one, 'λ' is wavelength of X-ray, 'β' is the full-width at half of the peak maximum in radians and 'θ' is Bragg's angle. The variation of the grain size with substrate temperature is shown in Table 1. Mismatch at inter-phase boundaries between crystalline lattices of film and substrate may develop stresses [12]. However, the stress has two components: (1) thermal stress arising from the difference of expansion coefficient of the film and substrate; and (2) internal stress due to the accumulating effect of the crystallographic flaws that are built into the film during

deposition [13]. Compressive stress is commonly observed in many deposited films. This is due to the grain boundary effect, which is predominant in polycrystalline film [13]. The origin of the strain is also related to the lattice misfit, which in turn depends upon the deposition conditions. The micro strain (ϵ) developed in the sprayed SnO₂ thin films was calculated from the equation

$$\epsilon = (1/\sin\theta) (\lambda/D - \beta\cos\theta) \dots\dots\dots (3)$$

Where ‘ β ’ is full-width at half-maximum of the (0 0 2) peak and ‘D’ is the average grain size; the calculated values are given in Table 1. It is observed that the micro strain (ϵ) exhibits a slow decreasing tendency up to about 450°C and afterwards increases at higher temperatures. This type of micro strain changes may be due to the predominant recrystallization process in the polycrystalline thin films. In fact, the growth mechanism involving dislocation is a matter of importance. Dislocations are imperfect in a crystal associated with the mis-registry of the lattice in one part of the crystal with respect to another part. Unlike, vacancies and interstitials atoms, dislocations are not equilibrium imperfections i.e., thermodynamic considerations are insufficient to account for their existence in the observed dislocation densities [14]. Dislocation density (δ) was determined using the relation and is given in Table 1. It is observed that δ decreases with temperature.

$$\delta = 1/D^2 \dots\dots\dots (4)$$

Table-I, II Micro structural Parameter of SnO₂ films

Temp (°C)	d _{std} (211)	d _{obs} (211)	a(Å)	c(Å)	D(nm)	$\epsilon \times 10^{-3}$	$\delta \times 10^{16}$ lines m ⁻²
350	1.735	1.737	4.73	3.15	10	4.56	1.00
375	1.735	1.739	4.74	3.16	15	4.47	0.44
400	1.735	1.741	4.74	3.17	18	4.41	0.30
450	1.735	1.740	4.72	3.18	21	4.45	0.22
525	1.735	1.741	4.73	3.18	25	4.89	0.16

The XPS survey scan spectra of the films heat treated at 525°C is shown in Fig.2. Fig 2(a) is the whole spectra; Fig (b) and Fig (c) are for Sn and O, respectively. It can be seen that the binding energy of Sn 3d_{5/2}, Sn 3d_{3/2} and O1s is 486.5, 494.9, and 530.6 eV, respectively, which is consistent with the results reported earlier [15]. The gap between the Sn 3d_{5/2} and Sn 3d_{3/2} levels (8.4 eV) is approximately the same as in the standard spectrum of Sn. On the other hand, the O 1s peak generally has been observed in the measured binding energy region of 529–535 eV and for chemisorbed O₂ on the metal surface the binding energy is found to be in the region 530–530.9 eV [16]. Therefore, the O 1s peak (530.6 eV) observed in the present work can be attributed to chemisorbed oxygen.

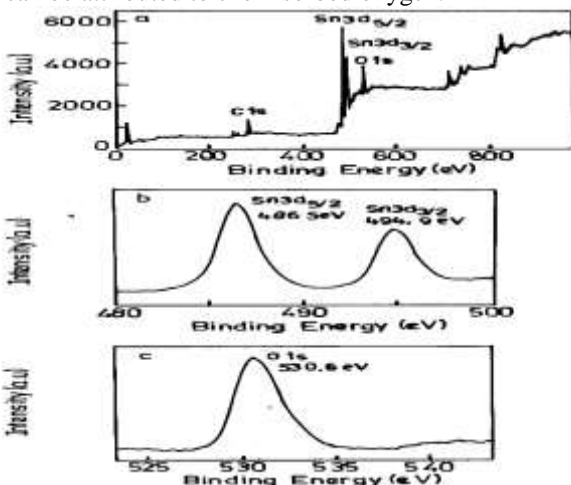


Fig.2 – XPS spectra of SnO₂ films heat treated at 525°C

The transmission spectra of the films heat treated at different temperatures is shown in Fig.3. The spectra exhibit interference fringes. The transmittance of the films is greater than 80 %. The refractive index was calculated using the interference maxima and minima observed at a wavelength from the transmission spectra by the envelope method [17] employing the following equations:

$$n = [N + (N^2 - n_s^2)]^2 \dots\dots\dots (5)$$

$$N = (n_s^2 + 1)/2 + 2n_s(T_{max} - T_{min})/T_{max} T_{min}$$

where n_s is the refractive index of the substrate, T_{max} and T_{min} are the maximum and minimum transmittances at the same wavelength in the fitted envelope curve on a transmittance spectrum. Fig.4 shows the variation of refractive index with wavelength. The refractive index of this film was in the range of 2.05 – 2.18. These values are in good agreement with the reported values [18]. The optical absorption co-efficient was calculated from Transmittance spectrum. A plot of (αhv)² vs. hv (Fig.5), indicated band gap value around 3.68 eV. Transport parameters like mobility and carrier density were obtained from Hall measurements. Resistivity was obtained by the four probe resistivity method. The resistivity of the films varying from 10⁻³ to 10⁻² ohm cm as the annealing temperature increased. Mobility values varied from 10 to 15 cm²v⁻¹s⁻¹. The carrier density values varied from 6.25 x 10²⁰ cm⁻³ to 4.1 x 10¹⁹ cm⁻³. The resistivity value is comparable with sputtered SnO₂ films [19].

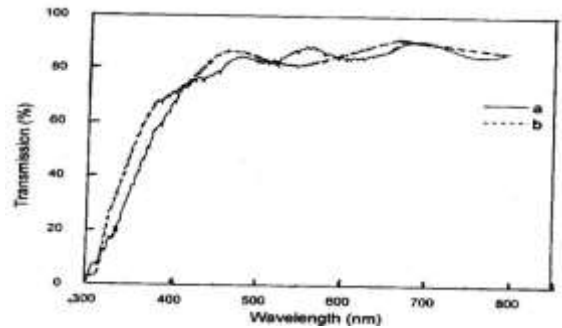


Fig.3 – Transmission spectra of SnO₂ films heat treated at different temperature (a)450°C (b)525°C

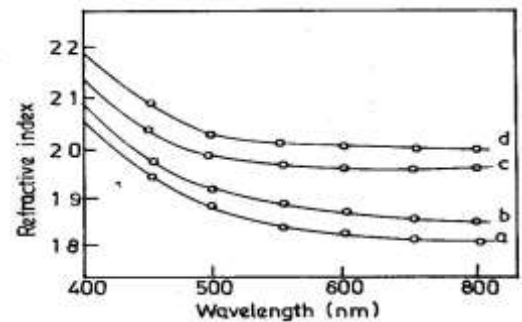


Fig.4 – Variation of Refractive index with wavelength of SnO₂ films heat treated at different temperatures (a) 350°C (b) 450°C (c) 500°C (d) 525°C

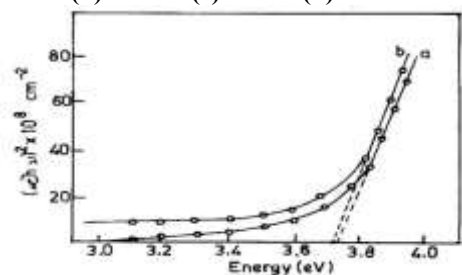


Fig.5– (αhv)² vs. hv plot of SnO₂ films post heat treated at (a) 450°C (b) 525°C

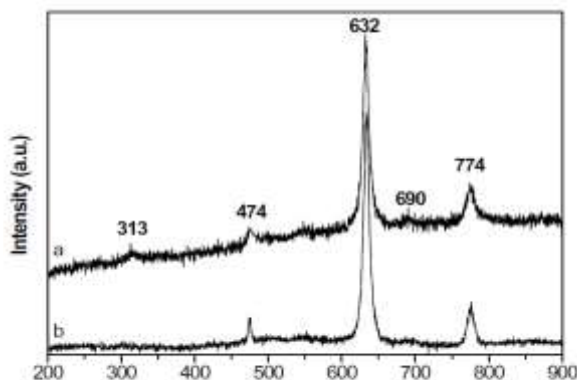


Fig.6– Raman spectrum of SnO₂ films heat treated at different temperature (a)450°C (b)525°C

Fig. 5 shows the room temperature Raman scattering spectra of the SnO₂ films heat treated at different temperatures. Three fundamental Raman peaks at 474, 632, and 774 cm⁻¹ corresponding to the E_g, A_{1g}, and B_{2g} vibration modes, respectively, are observed, in good agreement with those for the rutile bulk SnO₂. This result further confirms that the SnO₂ films deposited in this work possess the characteristics of the tetragonal rutile structure [19]. In addition to the fundamental Raman peaks of rutile SnO₂, the other two weak Raman peaks at about 313 and 690 cm⁻¹ are also observed, whereas these two Raman peaks are not detected in the SnO₂ films heat treated at 525°C (Fig.5b). This is similar to the results reported for rutile SnO₂ nanorods [20]. It is also observed that the three fundamental peaks of SnO₂ films are broadened for the films heat treated at 450°C, as compared with those of SnO₂ films heat treated at 525°C. The full width at half maximum (FWHM) of E_g, A_{1g}, and B_{2g} modes of SnO₂ films deposited at 450°C are 14.5, 9.3, and 13.8 cm⁻¹, respectively, while the FWHMs of the corresponding modes of films heat treated at 525°C are 4.0, 8.8, and 11.6 cm⁻¹, respectively. It is obvious that E_g mode is the broadest. The reasons are analyzed as following. Abello and co-workers [21] proposed that the relaxation of the $k > 0$ selection rule is progressive when the rate of disorder increases or the size decreases, and infrared (IR) modes can become weakly active when the structural changes induced by disorder and size effects take place. And also, it is well known that in an infinite perfect crystal only the phonons near the center of the Brillouin zone (BZ) contribute to the scattering of incident radiation due to the momentum conservation rule between phonons and incident light. As the crystallite is reduced to nanoscale, the phonon scattering will not be limited to the center of the Brillouin zone,

and phonon dispersion near the center of Brillouin zone must also be considered.

References

- [1] M. Sawada and M.Higuchi Thin solid films, 317 (1998) 157.
- [2] H.Y. Valencia, L.C.Moreno, A.M.Ardila, Microelectron.J.39 (2008) 1356.
- [3] H.M. Phillips, Y.Li, Z.Bi, B.Zhang, Appl.phys.A.63(1996) 347.
- [4] V.P.Godbole, .D.Vispute, S.M.Chaudhari , S.M.Kanetkar, S.B.Ogale, J.Mater.Res.5 (1990) 372.
- [5] R.Dolbec, M.A.ElKhakani, A.M.Serventi, M.Trudeau, R.G.Saint-Jacques, Thin Solid Films, 419 (2002) 230.
- [6] C.M.Ghimbeu, R.C.vanL and schoot, J.Schoonman, M.Lumbreras, J.Eur.Ceram.Soc 27 (2007) 207.
- [7] R.Khandelwal, A.P.Singh, A.Kapoor, S.Grigorescu, P.Miglietta, Opt.Laser Technol.41 (2009) 89.
- [8] S.Q.Zhao, Y.L.Zhou, S.F.Wang, K.Zhao, P.Han,RareMet 25 (2006) 693.
- [9] M.Kwoka, L.Ottaviano, M.Passacantando, G.Czempik, S.Santucci, J.Szuber, ppl. Surf.Sci.254 (2008) 8089 .
- [10] J.Kong, H.Deng, P.Yang, J.Chu,Mater. Chem.Phys.114 (2009) 854.
- [11] X.P.Cao, L.L.Cao, W.Q.Yao, X.Y.Ye, ThinSolidFilms, 317(1998) 443.
- [12]B.D.Cullity, Elements of X-ray Diffraction, A. W. Pub. Comp. Inc, (1978) 99 .
- [13] I.A. Ovid’Ko, Rev. Adv. Mater. Sci. (200) 61.
- [14] M. Bedir, M. Oztas, O.F. Bakkaloglu, R. Ormanel, Eur. Phys. J. B 45 (2005) 465.
- [15] J.Y.W. Seto, J. Appl. Phys. 46 (1975) 5247.
- [16] T.J. Ghuang, C.R. Brundle, D.W. Rice, Surf. Sci. 59 (1979) 413.
- [17] R.Swanepoel J.Phys.E, 16 (1983) 1214
- [18] D.Das, R.Banerjee, “Thin solid films, 147 (1987) 321.
- [19] J.J. Valenzuela Jauregui, R. Quintero Gonzalez, J. Hernandez Torres, A Mendoza Galva, R. Ramirez Bon, Vacuum, 76 (2004) 177.
- [20] W.Z. Wang, C.K. Xu, G.H. Wang, Y.K. Liu, C.L. Zheng, J. Appl. Phys. 92 (2002) 2740
- [21] Y.K. Liu, C.L. Zheng, W.Z. Wang, C.R. Yin, G.H. Wang, Adv. Mater. 13 (2001) 1883.
- [22] L. Abello, B. Bochu, A. Gaskov, S. Koudryavtseva, G.Lucazeau, M. Roumyantesva, J. Solid State Chem. 135 (1998) 78.